ANNALI DI GEOFISICA, VOL. 41, N. 3, August 1998

# A broadband two axis flux-gate magnetometer

**Paolo Palangio**
*Istituto Nazionale di Geofisica, Roma, Italy*

**Abstract**
A broadband two axis flux-gate magnetometer was developed to obtain high sensitivity in magnetotelluric measurements. In magnetotelluric sounding, natural low frequency electromagnetic fields are used to estimate the conductivity of the Earth's interior. Because variations in the natural magnetic field have small amplitude (10-100 pT) in the frequency range 1 Hz to 100 Hz, highly sensitive magnetic sensors are required. In magnetotelluric measurements two long and heavy solenoids, which must be installed, in the field station, perpendicular to each other (north-south and east-west) and levelled in the horizontal plane are used. The coil is a critical component in magnetotelluric measurements because very slight motions create noise voltages, particularly troublesome in wooded areas; generally the installation takes place in a shallow trench. Moreover the coil records the derivative of the variations rather than the magnetic field variations, consequently the transfer function (amplitude and phase) of this sensor is not constant throughout the frequency range 0.001-100 Hz. The instrument, developed at L'Aquila Geomagnetic Observatory, has a flat response in both amplitude and phase in the frequency band DC-100 Hz, in addition it has low weight, low power, small volume and it is easier to install in the field than induction magnetometers. The sensivity of this magnetometer is 10 pT rms.

**Key words** *flux-gate magnetometer*

## 1. Introduction

The flux-gate sensor is a non-linear system that can be represented as a black box with two inputs: the drive current and the ambient magnetic field. It produces an output that contains multiplicative and additive terms (fig. 1) of the input signals and the internal noise. The drive current is produced by means of a parametric oscillator (fig. 2). This device measures magnetic fields by utilizing the non linear characteristics of ferromagnetic material. The periodic saturation of the core produces even harmonic outputs that are approximately proportional to the ambient field. This process is described by a differential equation with time-varying coefficients.

There exist many theoretical studies of flux-gate mechanisms based on accurate descriptions of hysteresis and more complicated models for calculating the demagnetization which involve too many parameters that are difficult to evaluate for pratical designs. The flux-gate theory is complex, at this moment there is still no general solution for flux-gate equation.

The ferromagnetic material utilized in the ring core sensor is amorphous metal (vitrovac 6025). The amorphous metals (metallic glasses) are produced by rapid cooling of magnetic alloys consisting of iron, nickel, cobalt, boron and silicon. As a result of rapid cooling the material does not form a crystalline state but

*Mailing address*: Dr. Paolo Palangio, Istituto Nazionale di Geofisica, Via di Vigna Murata 605, 00143 Roma, Italy; e-mail: palangio@marte.ingrm.it

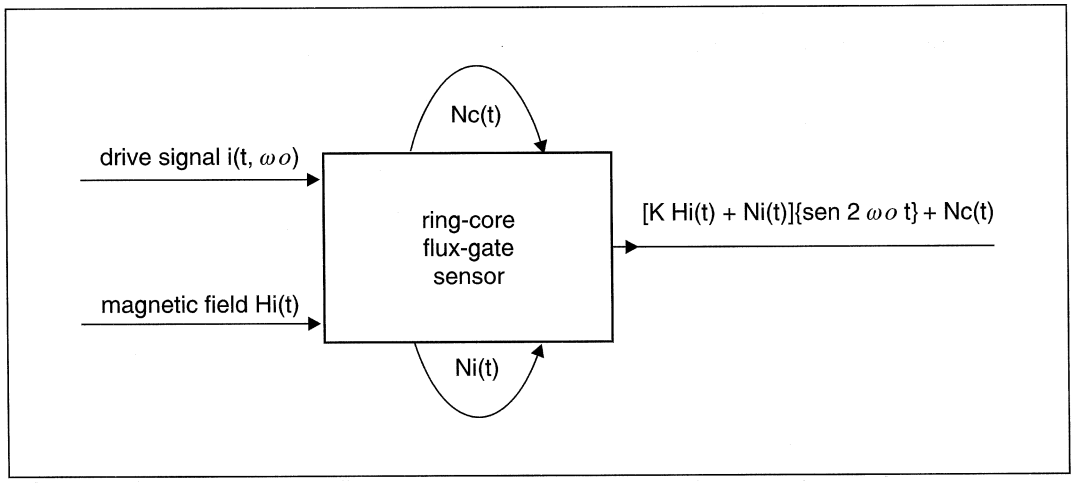


**Fig. 1.** Black box model flux-gate magnetometer.

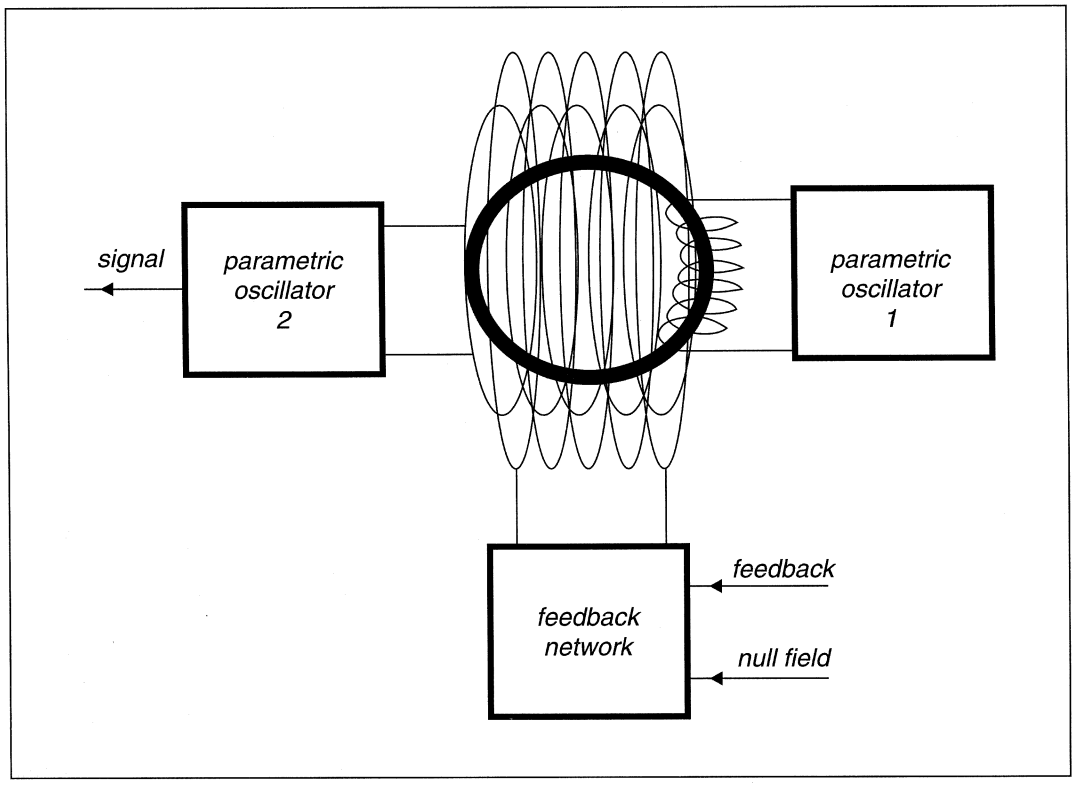


**Fig. 2.** Non linear oscillators.

instead produces a solid with only short range order with random microstructural properties. Vitrovac 6025 can be considered a random packing of spheres. The hysteresis loop of this material can be altered by annealing at intermediate temperatures (without leading to recrystallization) in the absence of magnetic field in order to change the shape of the hysteresis loop and to minimize the noise. The description of magnetization processes in this material is still far from a well established theoretical assessment, especially as regards the relation between physical processes and the details of the magnetization curves. The presence of a domain structure introduces a high level of complexity connected with inhomogeneities and structural disorder of the non magnetic part of the system. The magnetization loop is a multi-valued function of the driving external field and of the applied field-frequencies.

## 2. Flux-gate equation

The simplified flux-gate mechanism is based on the assumption that time varying inductance interacts with an external magnetic field. Therefore hysteresis, demagnetization, drive waveform and all dimensional quantities are included in the time varying inductance function (fig. 3), which is an observable quantity

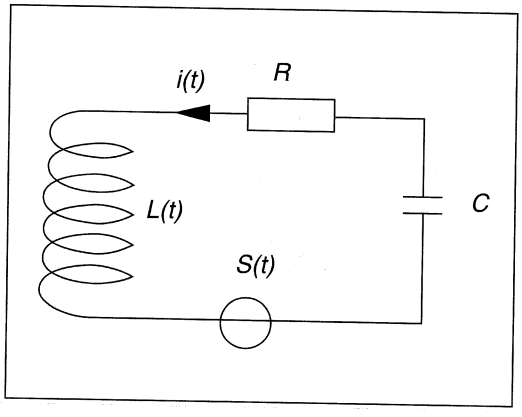


**Fig. 3.** Parametric oscillator 2.

(Primdahl *et al.*, 1994),

$$L(t) = KN^2 \frac{dB(t)}{dH_d(t)} + L_0$$

where $K$ is a constant which include all geometric parameters of the core, $N$ is the number of turns in the winding, $\frac{dB(t)}{dH_d(t)}$ is the differential permeability an $L_0$ is the self inductance of the winding without the core. For a full description of the simplified flux-gate mechanism, Lagrange equations can be derived (Goldstein, 1992), starting from the variational principle

$$\frac{d}{dt}\frac{\partial \mathcal{L}}{\partial q'} - \frac{\partial \mathcal{L}}{\partial q} + \frac{\partial D}{\partial q'} = S(t). \qquad (2.1)$$

Where $\mathcal{L}$ is the Lagrangian function ($T$-$V$) expressed in terms of the kinetic energy $T$ stored in the magnetic fields of the system (external field and internal field) and the potential energy $V$ stored in the capacitor

$$\mathcal{L} = \frac{1}{2}L(t)\left[\frac{dq}{dt}\right]^2 + \frac{l}{n}L(t)\,He\frac{dq}{dt} + \qquad (2.2)$$

$$+ M_{12}(t)\frac{dq}{dt}\frac{dq_d}{dt} - \frac{q^2}{2C}$$

where $He$ is the magnetic field to be measured, $n/l$ is the number of turns per unit length of the coil, $M_{12}$ is the mutual inductance between the drive coil and the sense coil, $i_d\left(\frac{dq_d}{dt}\right)$ is the drive current, $q$ is the electrical charge stored in the capacitor $C$.

The dissipative term is $D = \frac{1}{2}R\left[\frac{dq}{dt}\right]^2$. The resulting Lagrange equation ($M_{12} \cong 0$) is:

$$L(t)\frac{d^2q}{dt^2} + \frac{dq}{dt}\left[R + \frac{dL}{dt}\right] + \frac{d(t)}{C} = \qquad (2.3)$$

$$= S(t) - \frac{l}{n}\left[L(t)\frac{dHe}{dt} + He(t)\frac{dL(t)}{dt}\right]$$

which is a nonhomogeneous equation in the form

$$\frac{d^2q}{dt^2} + u(t)\frac{dq}{dt} + v(t)\,q(t) = G(t).$$

If $q_1(t)$ and $q_2(t)$ are two independent (linearly) solutions of the corresponding homogeneous simplified equation, the general solution is

$$q(t) = C_1 q_1(t) + C_2 q_2(t) +$$

$$+\{\int_{t_0}^{t} G(\xi)\, e^{p(\xi)} [q_1(\xi)\, q_2(t) + \qquad (2.4)$$

$$- q_1(t)\, q_2(\xi)]\, d\xi\}/W_0(q_1, q_2, t_0).$$

Where $W_0$ is the Wronskian of $q_1(t_0)$ and $q_2(t_0)$ and $p(\xi) = \int_{t_0}^{\xi} u(\varsigma)\, d\varsigma$.

Two linearly independent solutions can be (for $t_0 = 0$): $q_1(0) = 1$, $\frac{dq_1(0)}{dt} = 0$, $q_2(0) = 0$, $\frac{dq_2(0)}{dt} = 1$, hence $W_0 = 1$.

In order to simplify the solutions we assume that $u(t)$, $v(t)$ and $L(t)$ are periodic, the component measured by the sensor $He$ is constant (in the sense that $L(t)\frac{dHe}{dt} \ll He(t)\frac{dL}{dt}$) and $L(t)$ assumes only two values $L_h$ and $L_l$ (fig. 6). In consequence $q_1(t)$ and $q_2(t)$ are periodic: $q_1(t+\tau) = a_{11}q_1(t) + a_{12}q_2(t)$; $q_2(t+\tau) = a_{21}q_1(t) + a_{22}q_2(t)$; $q(t+\tau) = W(t)\,q(t)$.

The solutions are of the form $e^{\lambda t} z(t)$ where $\lambda$ is an eigenvalue of the Wronskian $W(t)$ and $z(t)$ is a periodic function which cannot be expressed in terms of the usual functions. When the real part of $\lambda$ is positive, the amplitude of the signal across $C$ grows indefinitely in time, the solution is unstable (Mitsubori and Saito, 1994). The time evolution of eq. (2.2) in the $\left[q(t), \frac{dq}{dt}\right]$ plane (Kouril and Vrba, 1988), features instability regions for many combinations of the sensor parameters and the phase of $L(t)$, that influence the eigenvalues of $W(t)$. In these instability ranges (Ohnishi and Inaba, 1994) the evolution paths are concentrated in small regions of the plane, and tiny perturbations can induce the system in a substantially different path. On the other hand, the high stability regions of the plane have low parametric amplification, resulting in a low sensitivity of the device.

As a consequence, care must be taken to select the values of the parameters with the assurance that thermal variations of the electronics components cannot drive the device in the instability regions.

The sensitivity of the sensor is maximum for $\frac{T_{L_h}}{T_{L_l}} = 1$ and it is roughly proportional to $\frac{L_h}{L_l}$ and to $\frac{2\omega_0 \langle L \rangle}{R}$.

## 3. Parametric amplification

In spite of discontinuity of $L(t)$ the Lagrangian term $\frac{d}{dt}\left(\frac{d\mathcal{L}}{dq'}\right) = \frac{d}{dt}\left[L(t)\frac{dq}{dt} + \frac{l}{n}HeL(t)\right]$ of eq. (2.1) must be continuous everywhere, at discontinuity $\frac{d}{dt}\left(\frac{d\mathcal{L}}{dq'}\right) = 0$; then $\Delta\left[L(t)\frac{dq}{dt}\right] = -\frac{l}{n}He \cdot \Delta[L(t)]$; there is a net increase in signal for each cycle, depending on the phase of the inductance changes. Figure 4 shows the mechanism of parametric amplification. Parametric amplification provides a means of

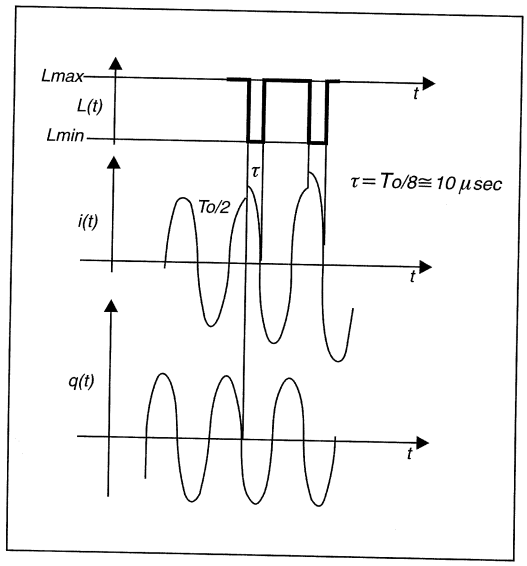


**Fig. 4.** Parametric amplification.

enhancing the second harmonic without degrading signal-to-noise ratio.

$L(t)$ is a periodic function of period $T = \pi/\omega$ made up of short impulses of length $\tau$ smaller than $T$ (fig. 4). $L(t)$ changes adiabatically, then some variables of the circuit can be adiabatically disregarded. The charge in the capacitor and the energy change very slowly when $L(t)$ goes from $L_h$ to $L_l$. The energy in the inductor cannot change during this short time therefore the current $i(t)$ will change: $\Delta i \approx 1\sqrt{\Delta L}$.

At the moment, when $i(t)$ attains maximum, $q(t)$ is zero. If $L(t)$ reachs its minimum value, $i(t)$ is modified, while $q(t)$ does not change appreciably. The net result is that the change in $L(t)$ increases the energy of the oscillator by multiplying it by a factor greater than 1. If the next impulsive change comes precisely at the moment in which $i(t)$ is again maximal, the oscillator will be destabilized.

The above process makes it possible to deliver permanent energy from the source changing the inductance to the resonant circuit. If the energy supplied to the circuit is greater than the energy dissipated in the resistor, the oscillations in the circuit will increase (Hagedorn, 1981).

## 4. Feedback loop

Since linearity and thermal drifts are related to the ambient magnetic field, we operate it in zero field, by means of a feedback loop. The feedback loop gain is implemented taking advantage of the non-linearity of the inductance of the signal coils. The inductance is time-dependent, so that we can build a parametric amplifier by means of a suitable capacitor in parallel to the secondary coil. We energize the second harmonic using power from the other harmonics. This technique allows us to amplify the second harmonic without introducing any additional noise.

The transfer function of the feedback loop (fig. 5) can be written as follows:

$$T(s) = \{S(s)A(s)/(1 + S(s)A(s)C(s)F(s))\}$$

where $S(s)$ is the transfer function of the sensor; $A(s)$ is the transfer function of the amplification chain, including the second harmonics filter, the synchronous detector and the integrator; $C(s)$ is the transfer function of the feedback circuit; $F(s)$ is the transfer function of the feedback network and coil. $T(s)$ can be expressed in a simple form (fig. 6) by means of the symmetric transfer matrix $[Tij] = \begin{bmatrix} T_{11} & T_{12} \\ T_{21} & T_{22} \end{bmatrix}$. The elements $Tij$ are the integrator time constant $RiCj$.

$$T(s) = (S_0 A_0/T_{11}T_{22})/\{s^2 + s[(T_{21} + T_{22})/T_{11}T_{22}] + S_0A_0/G_0T_{11}T_{22}\}$$

$G_0$, $F_0$, $S_0$ and $C_0$ are the values of the corresponding functions at $s = 0$, $A_0$ is the value of the function $A(s)$ at $s = j4\pi f_0$, $G_0 = F_0C_0$.

The natural frequency of the loop is

$$\omega = \sqrt{S_0A_0 / G_0T_{11}T_{22}};$$

the damping factor is

$$\zeta = (T_{21} + T_{22})\sqrt{G_0 / S_0A_0\, T_{11}T_{22}}$$

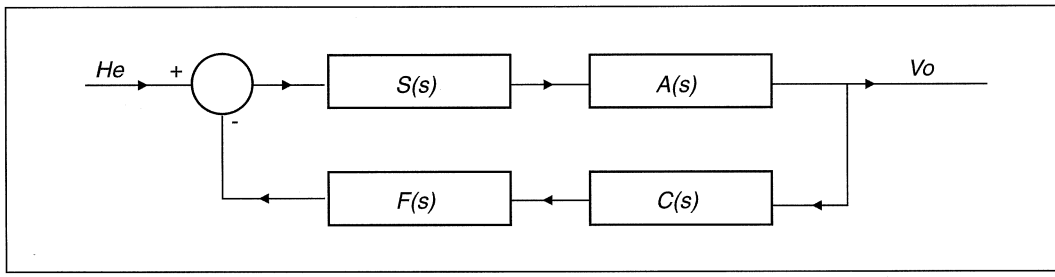


**Fig. 5.** Feedback loop.

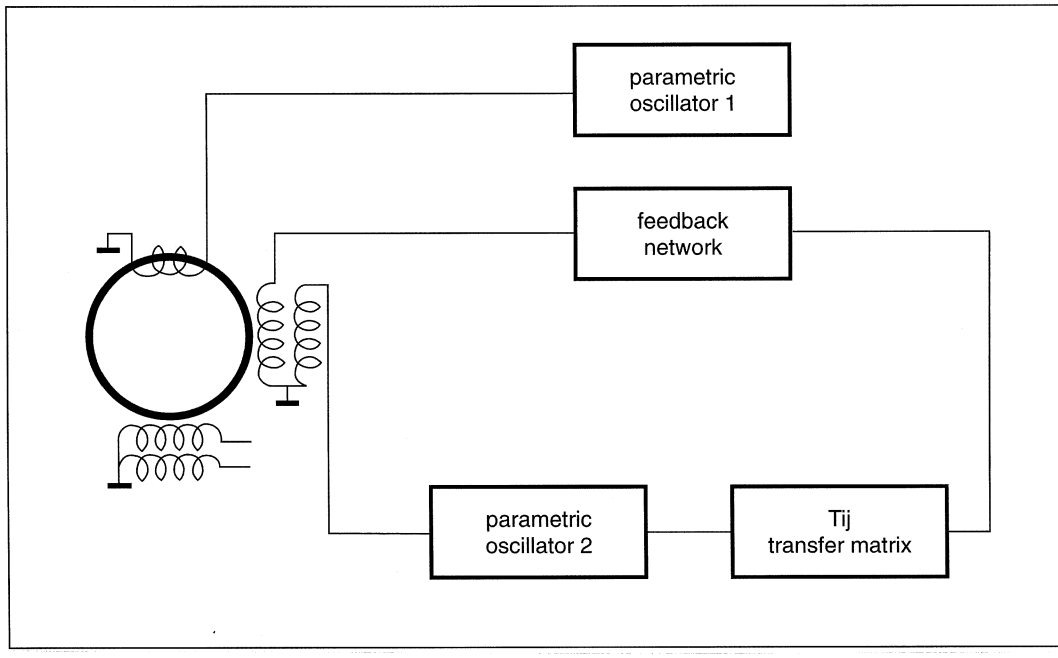


**Fig. 6.** Simplified circuit diagram for calculation of system transfer function.

and the noise bandwith is

$$B = \int_{-j\infty}^{+j\infty} T(s)\, ds$$

The main objective for the selection of circuits was the sensitivity performance of the devices to expected temperature perturbations of such parameters as the $R$ and $C$ elements; gains, offsets, and bandwith of the operational amplifiers.

## 5. Noise

The principal source of noise in a flux-gate magnetometer is produced within the core. The ferromagnetic material of the core exhibits

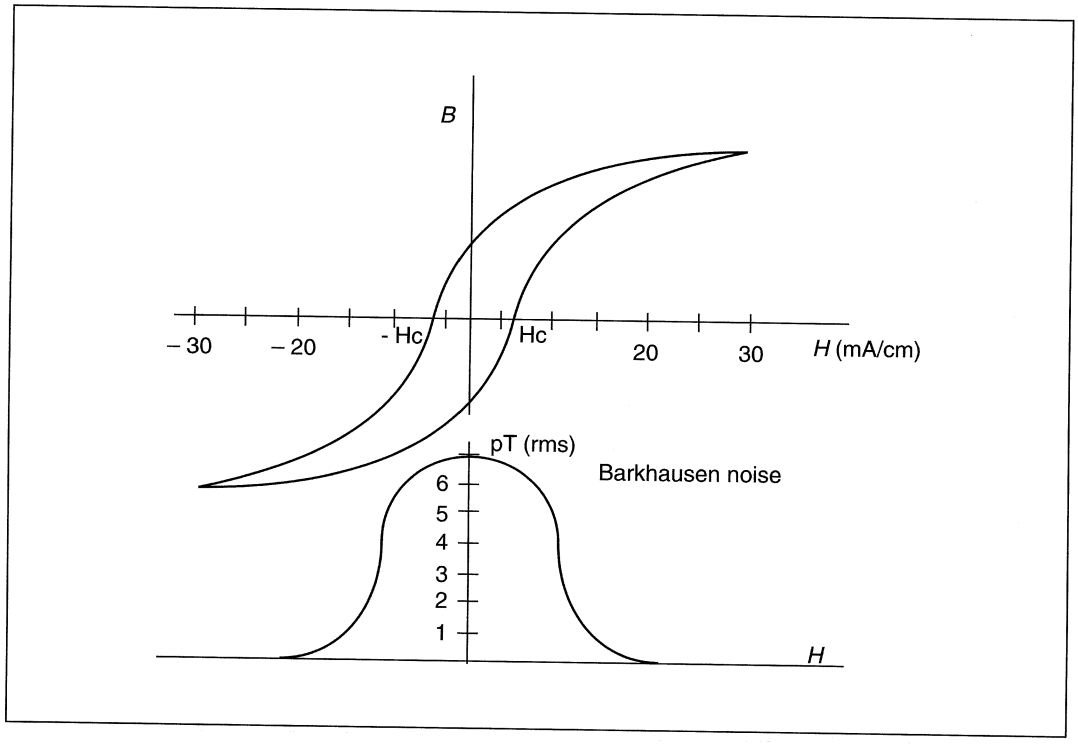


**Fig. 7.** Hysteresis loop and Barkhausen noise.

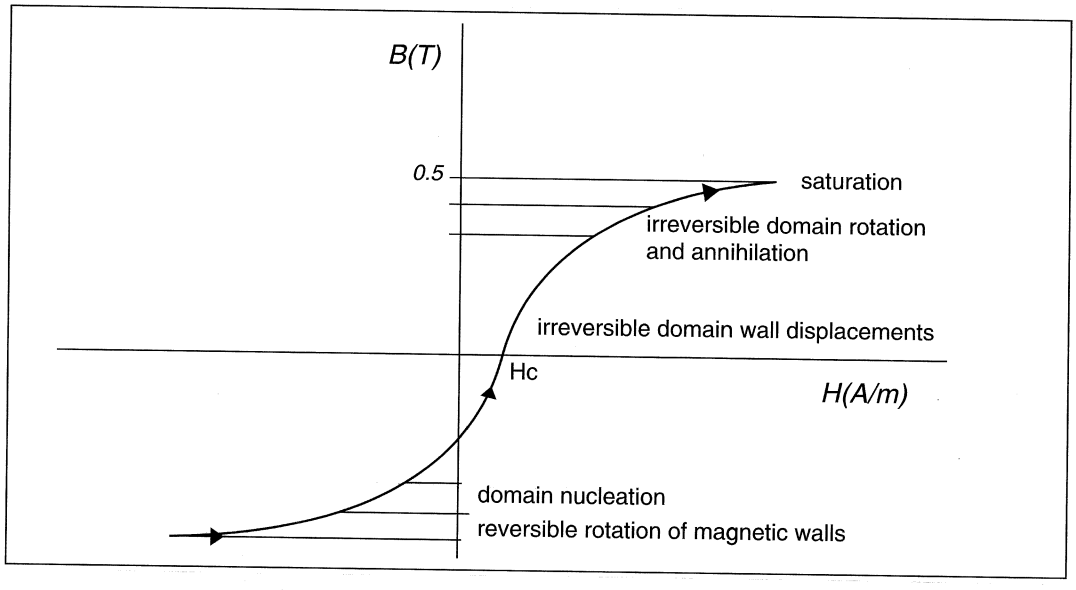


**Fig. 8.** Hysteresis loop and different magnetic processes.

three types of temporal random fluctuations of signal in flux-gate sensors:

1) Barkhausen noise.
2) Thermal noise.
3) Magnetostrictive noise.

Barkhausen noise originates from movement of domain walls (Scouten, 1970); it is due to a tendency to form clusters and jumps of magnetic domains. The maximum intensity of this noise is found near the coercitivity point (fig. 7). Figure 8 shows the hysteresis loop in which the different magnetic processes that give rise to Barkhausen noise are indicated: domain nucleation, 180° and 90° wall motion, domain annihilation.

The thermal or Nyquist noise is generated by the thermal energy of the conduction electrons and spin waves, acting on the domain configuration in ferromagnetic materials.

Magnetostrictive noise (Weiner, 1969) is due to random fluctuations of the magnetostrictive offset caused by frictional forces exceeding longitudinal magnetostriction of the core.

The Barkhausen noise (Dhar and Atherton, 1992) is minimized by reducing the time spent in the sections of the hysteresis loop where irreversible motions of the Bloch walls are produced. So that the major portion of the cycle is occupied by decreasing magnetization. The transition into saturation is carried out in a very short time (10 $\mu$s); this was achieved by means of a non linear oscillator (fig.9): in the high permeability section of the hysteresis loop the impedance of the thoroidal coil is large, and the capacitor $C$ is charged through the inductor $L$; when the core reaches the saturation the impedance of the thoroidal coil becomes small, and the energy stored in the capacitor is transferred to the saturated inductance of the excitation coil, producing a large current pulse (some Amps in a few $\mu$s).

The core wasade of amorphous magnetic ribbon with a width of 2 mm and thickness of 25 $\mu$m, wound in 10 layers around a ring.

In order to minimize the friction between ribbon layers, the tape was embedded in hydrocarbon based ferrofluid.

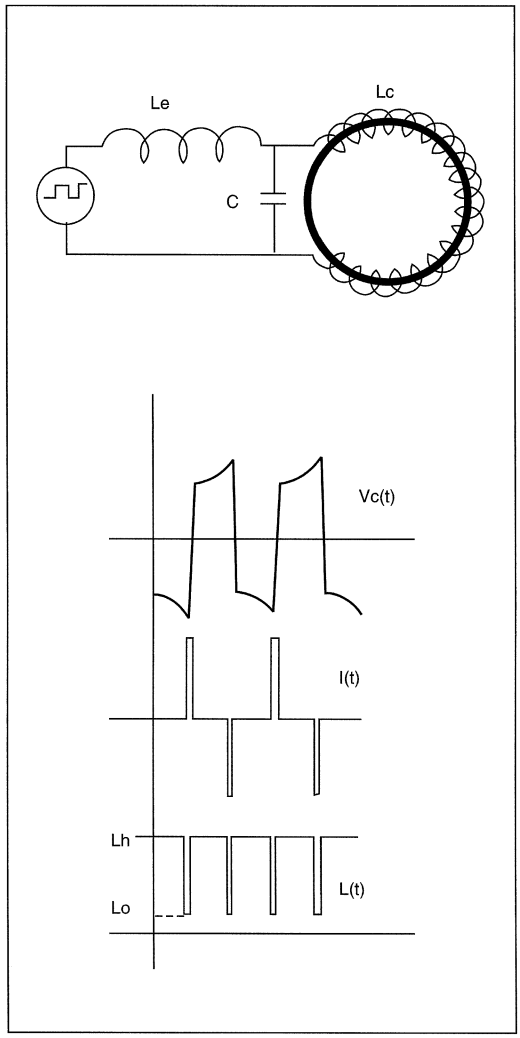


**Fig. 9.** Parametric oscillator 1 and drive waveforms.

## 6. Conclusions

The magnetometer developed at L'Aquila Geomagnetic Observatory allows (fig. 10) continuous recording of two components of the horizontal magnetic field in the frequency band DC-100 Hz. This instrument, developed for magnetotelluric measurements, is compact, inexpensive, low-power and portable. The output

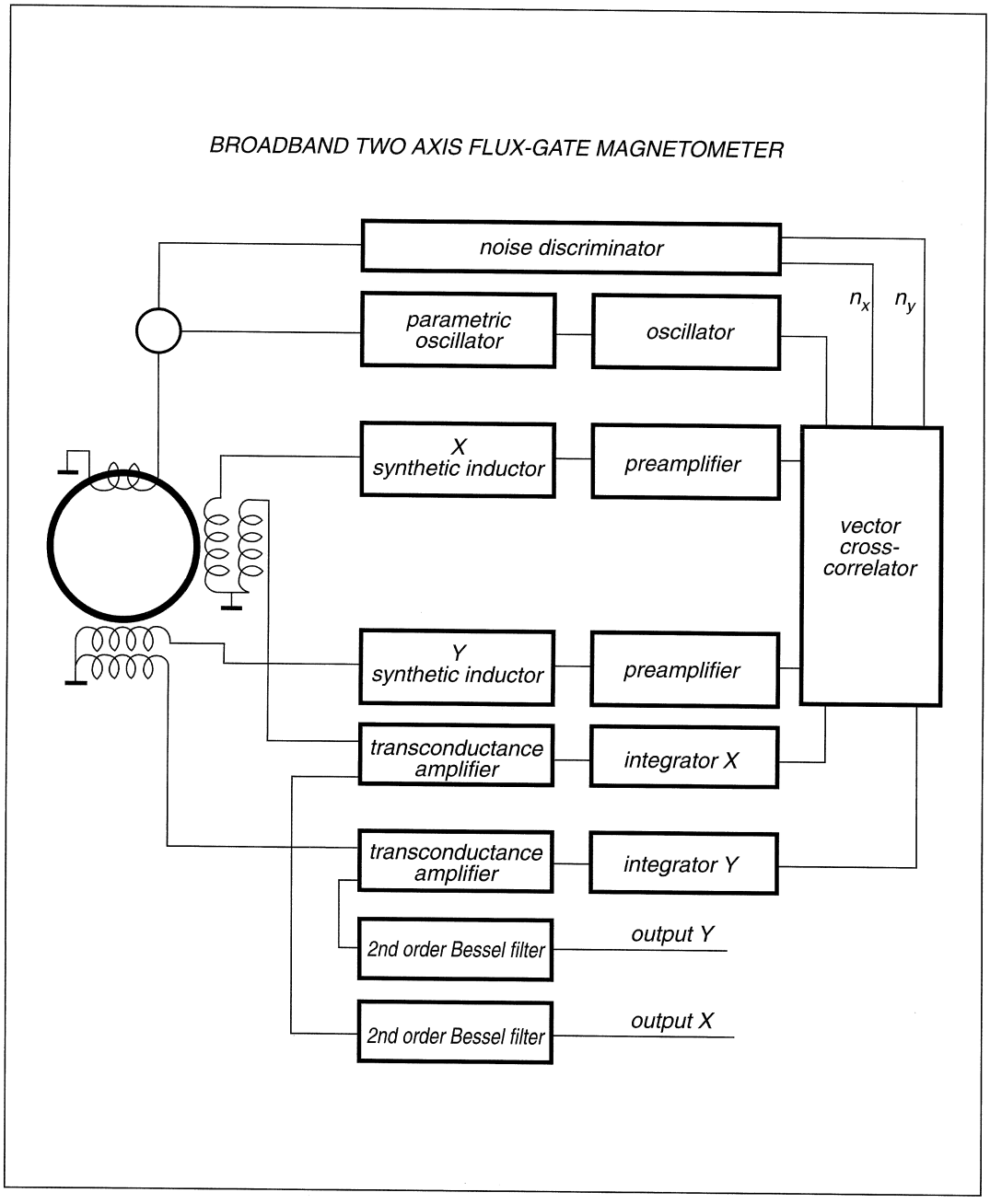


**Fig. 10.** Block diagram of the device.

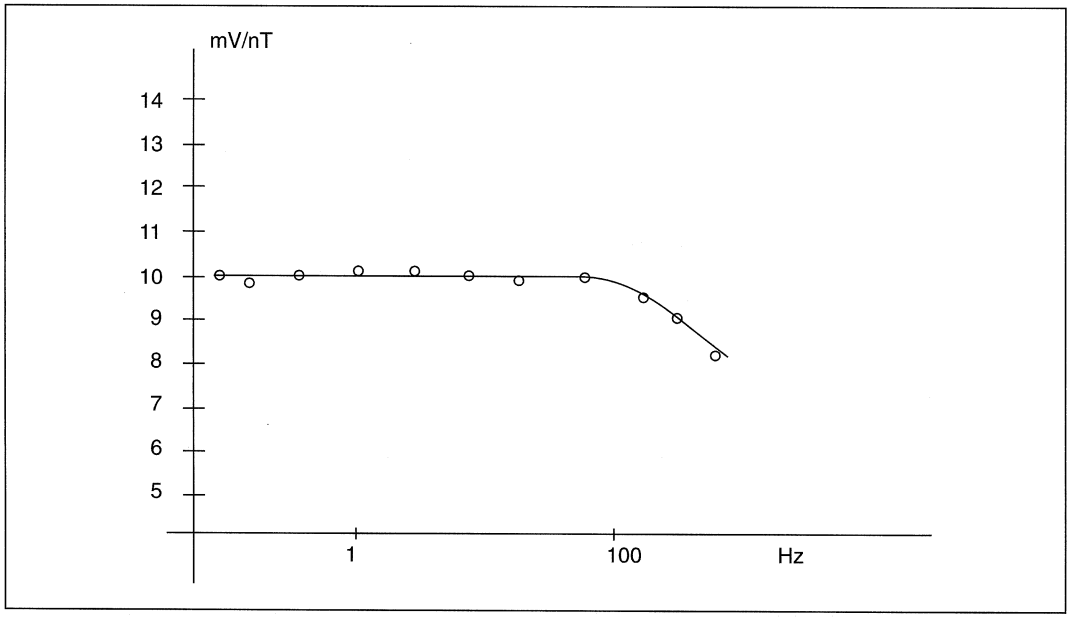


**Fig. 11.** Transfer function.

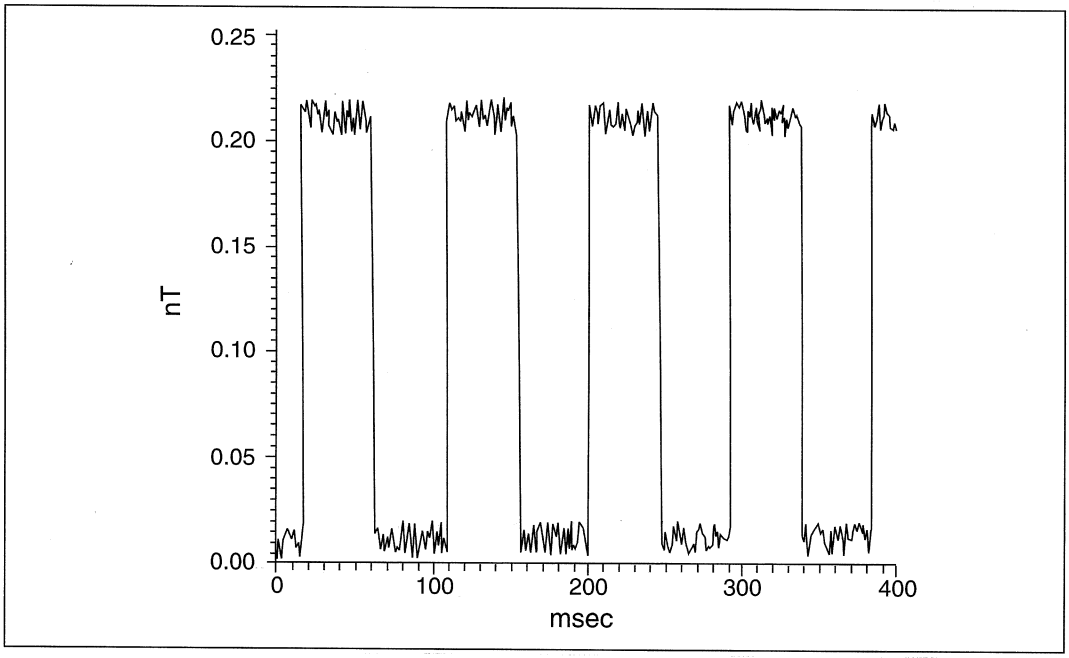


**Fig. 12.** Time response to square wave.

signal of this instrument does not need deconvolution processes to obtain true agnetic field values because it has a flat response in the entire frequency range (fig. 11), fig. 12 shows the time response to square waves.

## Acknowledgements

I am most grateful to F. Biasini, C. Gizzi and I. Settembrini for making the sensor devices.

*REFERENCES*

DHAR, A. and D.L. ATHERTON (1992): Influence of magnetizing parameters on the magnetic Barkhausen noise, *IEEE Trans. Magn.*, **28** (6), 3363-3366.

GOLDSTEIN, H. (1992): *Meccanica Classica* (Zanichelli, Bologna), 42-47.

HAGEDORN, P. (1981): *Non Linear Oscillations* (Clarendon Press-Oxford), 117-151.

KOURIL, F. and K. VRBA (1988): *Non-linear Parametric Circuits* (John Wiley & Sons), 73-184.

MITSUBORI, K. and T. SAITO (1994): A four dimensional plus hysteresis chaos generator, *IEEE Trans. Circuits Syst.*, **41** (12), 782-788.

OHNISHI, M. and N. INABA (1994): A singular bifurcation into istant chaos in a piecewise-linear circuit, *IEEE Trans. Circuits Syst.*, **41** (6), 433-442.

PRIMDAHL, F., B. HERNANDO, J.R. PETERSEN and O.V. NIELSEN (1994): Digital detection of flux-gate sensor output signal, *Meas. Sci. Technol.*, **5**, 359-362.

SCOUTEN, D.C. (1970): Barkhausen discontinuities in the saturation region, *IEEE Trans. Magn.*, **6** (2), 383-385.

WEINER, M.M. (1969): Magnetostrictive offset and noise in flux-gate magnetometer, *IEEE Trans. Magn.*, **5** (2), 98-105.